Tuning Long-Range Fermion-Mediated Interactions in Cold-Atom Quantum Simulators

Javier Argüello-Luengo[1,*] Alejandro González-Tudela[2,†] and Daniel González-Cuadra[3,4,‡]

[1]*ICFO—Institut de Ciències Fotòniques, The Barcelona Institute of Science and Technology,*
Avinguda Carl Friedrich Gauss 3, 08860 Castelldefels (Barcelona), Spain
[2]*Institute of Fundamental Physics IFF-CSIC, Calle Serrano 113b, 28006 Madrid, Spain*
[3]*Institute for Theoretical Physics, University of Innsbruck, 6020 Innsbruck, Austria*
[4]*Institute for Quantum Optics and Quantum Information of the Austrian Academy of Sciences, 6020 Innsbruck, Austria*

Engineering long-range interactions in cold-atom quantum simulators can lead to exotic quantum many-body behavior. Fermionic atoms in ultracold atomic mixtures can act as mediators, giving rise to long-range Ruderman-Kittel-Kasuya-Yosida–type interactions characterized by the dimensionality and density of the fermionic gas. Here, we propose several tuning knobs, accessible in current experimental platforms, that allow one to further control the range and shape of the mediated interactions, extending the existing quantum simulation toolbox. In particular, we include an additional optical lattice for the fermionic mediator, as well as anisotropic traps to change its dimensionality in a continuous manner. This allows us to interpolate between power-law and exponential decays, introducing an effective cutoff for the interaction range, as well as to tune the relative interaction strengths at different distances. Finally, we show how our approach allows one to investigate frustrated regimes that were not previously accessible, where symmetry-protected topological phases as well as chiral spin liquids emerge.

Introduction.—Long-range interactions between ultracold atoms are known to be the source of exotic many-body phenomena, including supersolid [1–6], magnetic [7–12], and topological phases [13–23], soliton trains [24–27], quantum droplets [28–30], or roton spectra [31,32]. Besides, if the long-range interactions appear between fermionic atoms, they can be harnessed to build analog simulators for quantum chemistry [33–35] and high-energy physics [36–39]. Unfortunately, these interactions do not appear naturally between neutral atoms, since they generally interact through (local) elastic collisions [40]. This is why finding ways to engineer and control effectively such long-range atomic interactions is one of the most pressing issues in atomic physics today.

As it occurs in nature, a conventional way of obtaining long-range interactions is through the exchange of mediating particles. For example, the exchange of photons through the atomic optical transitions leads to dipolar interactions $(1/r^3)$ in the case of highly magnetic [41–43] and Rydberg atoms [44–47], or dipolar molecules [48–51]. One can extend their range by shaping the photonic field with cavities [31,52–55] or nanophotonic structures [56–58]. However, such photon-mediated interactions are accompanied by dissipation, which needs to be controlled to profit from them. An orthogonal direction that is recently being considered consists in using fermionic atoms in atomic mixtures as mediators [26,32,59–75]. Such fermion-mediated interactions have been predicted [66,67,76] to lead to the Ruderman-Kittel-Kasuya-Yosida (RKKY)-type

interactions appearing in solids [77–79], which have a power-law, oscillating nature, fixed by the dimensionality and density of the Fermi gas. With the recent experimental observation of such interactions [26,69], a timely question that has been scarcely explored [32] is how one can further tune those interactions to be able to explore new phenomenology with them.

In this Letter, we take advantage of the flexibility offered by ultracold atomic platforms to control the range and shape of long-range fermion-mediated interactions, going beyond the conventional RKKY-type interactions encountered in solid-state systems. This allows us to design a quantum simulation toolbox that can be used to prepare, for instance, frustrated phases that are not accessible using other approaches. The Letter is organized as follows. First, we review how to derive the effective fermion-mediated RKKY interactions for a Fermi-Bose mixture of ultracold atoms. We then introduce an additional optical potential for the Fermi gas and show how the range of the interactions can be interpolated from a power law to an exponential decay by tuning the ratio between the periodic potential and the confining harmonic trap. This allows one at the same time to select the ratios between interactions at different distances within a nonvanishing range. We then show how, for a hardcore bosonic chain immersed in the fermionic cloud, the resulting interactions can be used to prepare frustrated phases with nontrivial topological properties. Finally, we explore an extra tuning knob by continuously changing the dimensionality of the cloud using different

083401-1

harmonic frequencies in each spatial direction. This control allows one to further tune the interaction ratios that, as we indicate, might be useful to obtain 2D chiral spin liquid phases [80].

Effective fermion-mediated interactions.—Let us consider an atomic mixture as depicted in Fig. 1(a), where one species corresponds to noninteracting spinless fermions trapped by a harmonic potential,

$$V(x, y, z) = \frac{m_f}{2}[\omega_x^2 x^2 + \omega_y^2 y^2 + \omega_z^2 z^2]. \quad (1)$$

The fermionic Hamiltonian reads $\hat{H}_f = \sum_n \varepsilon_n \hat{c}_n^\dagger \hat{c}_n$, where $\hat{c}_n^{(\dagger)}$ is the (creation) annihilation operators associated with the nth eigenstate of this oscillator, with energy ε_n. For concreteness, and without lack of generality, we assume that the other atomic species is bosonic and it is trapped in an optical lattice, $V_{\text{lat}}(\boldsymbol{r})$, with fixed lattice spacing d. While Pauli blocking prevents s-wave interactions among spin-polarized fermions, one can still account for boson-boson and boson-fermion collisions. This leads to a bosonic Hamiltonian of the form

$$\hat{H}_b = \int d\boldsymbol{r}\, \hat{\phi}^\dagger(\boldsymbol{r})\left[\frac{-\hbar^2}{2m_b}\nabla^2 + V_{\text{lat}}(\boldsymbol{r})\right]\phi(\boldsymbol{r})$$
$$+ g_{\text{bb}}\int d\boldsymbol{r}\, \hat{\phi}^\dagger(\boldsymbol{r})\hat{\phi}^\dagger(\boldsymbol{r})\hat{\phi}(\boldsymbol{r})\hat{\phi}(\boldsymbol{r}), \quad (2)$$
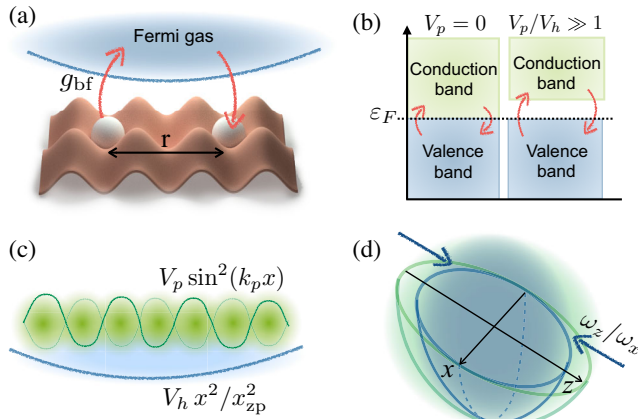

FIG. 1. (a) Two bosonic atoms (white) separated by distance r and trapped in an optical lattice (red) experience an effective long-range interaction mediated by a Fermi gas trapped in an harmonic potential (blue). (b) The contact Bose-Fermi interactions (g_{bf}) virtually populates the conduction band of the Fermi gas. (c) An additional oscillatory potential induces a gap between the valence and conduction gap, exponentially damping the mediated interactions. (d) By controlling the strength of the trapping potential in an orthogonal direction, ω_z/ω_x, one can continuously tune the dimension of the Fermi gas from 1D to 2D, introducing additional modulating frequencies, as will be shown in Fig. 4.

and a Bose-Fermi density-density interaction,

$$\hat{H}_I = g_{\text{bf}}\int d\boldsymbol{r}\, \hat{\phi}^\dagger(\boldsymbol{r})\hat{\psi}^\dagger(\boldsymbol{r})\hat{\phi}(\boldsymbol{r})\hat{\psi}(\boldsymbol{r}), \quad (3)$$

where the field operator $\hat{\phi}(\boldsymbol{r})[\hat{\psi}(\boldsymbol{r})]$ describes the annihilation of a boson [fermion] and $g_{\text{bb}}(g_{\text{bf}})$ is the bosonic (interspecies) coupling constant, which is experimentally tunable through magnetic Feshbach resonances [81].

Below the Fermi temperature, the N fermionic atoms are occupying all states up to the Fermi energy, $\varepsilon_F = \varepsilon_N$, and the state can then be written as $|\Omega\rangle = \prod_{n=1}^N \hat{c}_n^\dagger|0\rangle$. In the regime where fermionic timescales are much faster than the bosonic ones and their interaction is weak, one can take $\hat{H}_0 = \hat{H}_b + \hat{H}_f$ as the unperturbed Hamiltonian and $\hat{H}_I$ as a perturbation, obtaining an effective potential for the bosons [66],

$$\hat{H}_{\text{eff}} = \varepsilon_F + \hat{H}_b + G\iint d\boldsymbol{r}d\boldsymbol{r}'\, F_{\boldsymbol{r},\boldsymbol{r}'}\hat{\phi}^\dagger(\boldsymbol{r})\hat{\phi}^\dagger(\boldsymbol{r}')\hat{\phi}(\boldsymbol{r})\hat{\phi}(\boldsymbol{r}'),$$
$$(4)$$

where $G = 2m_f g_{bf}^2 k_F^4/\hbar^2$, and we define the Fermi momentum $k_F = \sqrt{2m_f \varepsilon_F}/\hbar$. Here, the last term arises from the second-order perturbation $\sum_{m\neq i}|\langle m|\hat{H}_I|i\rangle|^2/(E_m - \varepsilon_F)$, where the initial state $|i\rangle = |\Omega\rangle|\{r_b\}\rangle$ belongs to the ground-state manifold of $\hat{H}_0$ for bosonic atoms placed in positions $\{r_b\}$, and $|m\rangle = \hat{c}_m^\dagger \hat{c}_n|\Omega\rangle|\{r_b\}\rangle$ is a particle-hole excited state outside the manifold, with energy E_m. Note that due to the conservation of fermionic parity, fermions needs to be exchanged twice to generate a potential, unlike photons that can be exchanged only once. This has important implications for the sign and shape of $F_{\boldsymbol{r},\boldsymbol{r}'}$ [82], which in this case only depends on the bosonic separation $F_{\boldsymbol{r},\boldsymbol{r}'} \approx F(|\boldsymbol{r} - \boldsymbol{r}'|)$.

Since it will be useful to interpret the results of this Letter, let us review here the properties of an untrapped free Fermi gas with energy dispersion $\varepsilon_{\boldsymbol{k}}^0 = (\hbar^2|\boldsymbol{k}|^2/2m_f)$, which provides a first approximation in the limit $N \gg 1$. Analytical expressions in this limit can be found in all spatial dimensions [78,83,84]. For example, in the one-dimensional case ($N\omega_x \ll \omega_{y,z}$), $F(r)$ expands in the limit $k_F r \gg 1$ as [83]

$$F_{\text{1D}}(r) \propto \frac{-1}{k_F r}\left[\cos(2k_F r) + \frac{\sin(2k_F r)}{2k_F r}\right], \quad (5)$$

whereas in the two-dimensional case ($\omega_x = \omega_z \ll \omega_y/N$), it expands as [84]

$$F_{\text{2D}}(\boldsymbol{r}) \propto -\frac{1}{k_F^2 r^2}\left[\sin(2k_F r) - \frac{\cos(2k_F r)}{4k_F r}\right]. \quad (6)$$

In both dimensions, the interactions share some common features: (i) the fermion-mediated interactions are attractive

in the limit $r \to 0$, regardless of the sign of g_{bf}. The mean-field intuition is that, for $g_{bf} > (<)0$, the Fermi gas tends to avoid (be attracted to) the bosons, reducing (increasing) the fermionic density, and thus, the bosons feel more attracted to this place. (ii) Asymptotically, they lead to longer range interactions $\sim r^{-1}$ (1D) and $\sim r^{-2}$ (2D) than dipolar ones ($\sim r^{-3}$). (iii) The interactions oscillate with an effective length inversely proportional to k_F. Thus, choosing the wave vector of the bosonic optical lattice potential k_L, one can induce (anti)ferromagnetic interactions if $k_L = (2)k_F$, or incommensurate ones ($k_L/k_F \in \mathbb{I}$).

For a sufficiently deep optical lattice for the bosons, only its lowest motional bands get populated. Wannier functions $w_j(\mathbf{r})$ centered at the lattice sites j become a convenient description for the bosonic fields, $\hat{\phi}(\mathbf{r}) = \sum_j w_j(\mathbf{r})\hat{b}_j$ [85]. Projecting in this basis the effective Hamiltonian of Eq. (4), one obtains an extended Bose-Hubbard model:

$$\hat{H}_{\text{eff}} = -t_b \sum_{\langle j,j' \rangle} \hat{b}_j^\dagger \hat{b}_{j'} + \frac{U_b}{2} \sum_j \hat{n}_j^b(\hat{n}_j^b - 1) + \sum_{j,j'} v_{j,j'} \hat{n}_j^b \hat{n}_{j'}^b,$$

(7)

with nearest-neighbor tunneling strength t_b and on-site interaction $U_b = g_{bb} \int d\mathbf{r} |w_j(\mathbf{r})|^4$, where t_b, $\max |v_{j,j'}| \ll \hbar\omega_{x,y,z}$ to satisfy the previous perturbative treatment. Here, $\hat{b}_j^{(\dagger)}$ are the (creation) annihilation operators of a bosonic atom on site j, $\hat{n}_j^b = \hat{b}_j^\dagger \hat{b}_j$ is the bosonic number operator, and the effective potential $v_{j,j'}$ terms can be obtained from the perturbed potential of Eq. (4) as

$$v_{j,j'} = G \iint d\mathbf{r} d\mathbf{r}' \, F(|\mathbf{r} - \mathbf{r}'|)|w_j(\mathbf{r})|^2 |w_{j'}(\mathbf{r}')|^2. \quad (8)$$

Controlling the range of the interactions.—We now show how the range of the effective interactions can be controlled by adding a periodic potential $V_p \sin^2(k_p x)$ to the previous fermionic trap in the 1D case, $V(x) = V_h \cdot (x/x_{zp})^2$, where $V_h = \hbar\omega_x/4$ and $x_{zp} = [\hbar/(2m_f\omega_x)]^{1/2}$, as illustrated in Fig. 1(c). In the following, we fix the number of fermionic atoms, while we vary the ratio V_p/V_h by modifying the depth of the periodic potential. It is expected that a value of $V_p \neq 0$ opens up a gap in the energy dispersion of the fermionic excitations, introducing a cutoff in the interaction range if the Fermi energy lies within the band gap [see Fig. 1(b)]. This is guaranteed by choosing an appropriate wave vector k_p for the fermionic optical lattice, such that $k_p x_{zp} \sim \sqrt{N}$ and the oscillatory potential maximally hybridizes with the $N - 1$ nodes of the highest occupied state.

In Fig. 2(a), we show the fermion-mediated interaction appearing in a 1D Fermi gas for two values of V_p/V_h corresponding to the pure harmonic case ($V_p/V_h = 0$, dashed green) and a ratio $V_p/V_h = 400$ (solid red). We observe how the periodic potential tends to (exponentially)
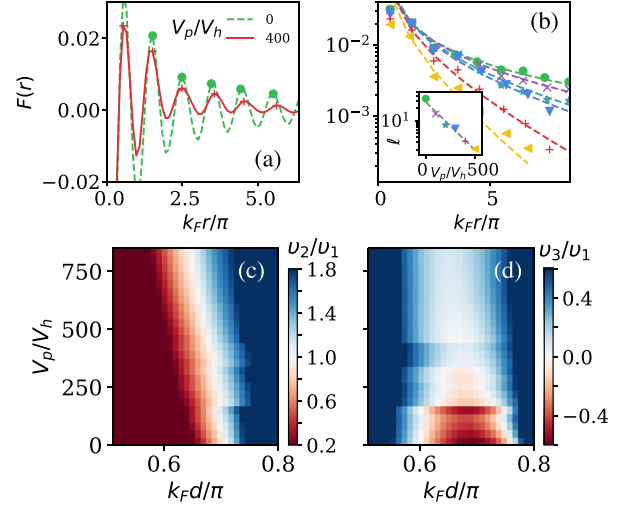

FIG. 2. (a) Effective potential between two atoms in one dimension mediated by a Fermi gas trapped in an harmonic trap with (green) and without (red) an extra periodic trap of strength $V_p/V_h = 400$. Markers indicate the oscillation maxima. (b) Value of the maxima for increasing values of V_p/V_h. The inset shows the decay length ℓ of a fitted Yukawa interaction, $\sim \exp[-k_F r/(\pi\ell)]/r$. (c–d) Strength of the second v_2/v_1 (c) and third v_3/v_1 (d) neighbor interactions as a function of V_p/V_h and the effective lattice spacing $k_F d$. Here, the bosonic Wannier function $w_j(\mathbf{r})$ is approximated by a gaussian distribution with, $x_{\text{width}}/d = 0.17$, consistent with a lattice wavelength $\lambda = 784.7$ nm for ^{87}Rb. See Ref. [85] for a more thorough discussion about the experimental parameters chosen for this and the rest of the figures.

cut the range of the interaction, inducing a purely positive potential for distances $k_F r > 2$. In Fig. 2(b), we plot the maximum relative values of the fermion-mediated interactions at the oscillations for increasing values of V_p/V_h, where it is more evident the transition from a power-law decay for small V_p/V_h to an exponentially decaying Yukawa-like interaction when V_p/V_h is large. We can therefore control the effective interaction range, given by the exponential decay length ℓ, which is exponentially reduced by the introduced gap $\sim V_p/V_h$, as $\ell \sim e^{-\alpha V_p/V_h}$ (inset) [85].

Besides, playing with the effective lattice separation of the bosonic species $k_F d$ (which can be controlled through the frequency of the harmonic trap, adjusting k_p accordingly), one can identify diverse choices of induced interactions, as we illustrate in Figs. 2(c) and 2(d). There, we see for example that there are regions for V_p/V_h and $k_F d$ (colored in white) where the potential for the nearest and next-nearest neighbors coincide $v_2 \approx v_1$, while interactions among longer distance atoms are very weak, $v_3/v_1 \approx 0$. This is important, as such potentials can be the source of frustrated quantum many-body phases.

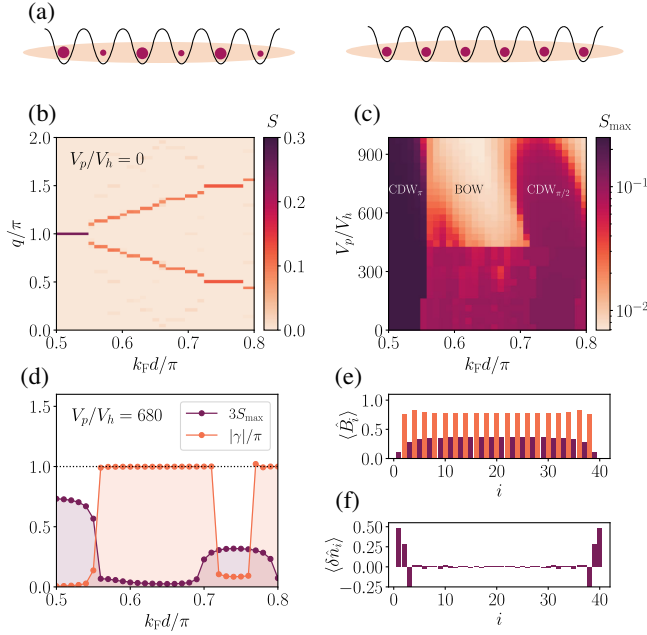*Quantum simulation toolbox for frustrated phases.*—To illustrate the last point, we analyze the phase diagram of a

FIG. 3. (a) Real-space configuration of the CDW_π (left), where spheres of different sizes correspond to an alternating atomic occupation, and frustrated BOW (right) with a dimerized bond structure. (b) $S(q)$ as a function of $k_F d$ for a chain with $L = 60$ sites and bosonic density $\rho = 1/2$, for $V_p = 0$. The phase diagram presents a staircase structure, where every step corresponds to a CDW_q characterized by a peak in $S(q)$. (c) Value of S at the peak, S_{max} as a function of $k_F d$ and V_p/V_h, showing how the CDW orders melt for sufficiently large values of V_p/V_h, giving rise to a frustrated BOW. (d) S_{max} and Berry phase γ as a function of $k_F d$ for $V_p/V_h = 680$, showing the nontrivial topological nature of the BOW phase. Real-space configuration of the BOW phase for $L = 40$, showing (e) dimerized bonds and (f) localized edge states at the boundaries. Parameters as in Fig. 2.

1D chain of hardcore bosons ($U_b/t_b \to \infty$) whose interactions are mediated by a 1D Fermi gas. The different phases can be distinguished using the structure factor, $S(q) = (1/L^2) \sum_{i,j} \langle \delta \hat{n}_i^b \delta \hat{n}_j^b \rangle e^{iq(r_i - r_j)}$, where $\delta \hat{n}_i^b = \hat{n}_i^b - \rho$ and $\rho = 1/L \sum_i \langle \hat{n}_i^b \rangle$ is the bosonic density.

Using a density-matrix renormalization group algorithm [94] with fixed bond dimension $D = 200$, we calculate the 0-temperature ground state of a periodic chain with $L = 60$ sites and half-occupation, $\rho = 1/2$. Figure 3(b) shows how, for $V_p/V_h = 0$, $S(q)$ develops a clear peak at a certain value q_0 that varies with $k_F d$. The value at the peak $S_{max} = S(q_0)$ can be used as an order parameter, revealing in this case a staircase structure where every step corresponds to a charge-density wave (CDW) phase with long-range order in the atomic density. For each of them, the order is characterized by the momentum q_0, and we labeled these phases as CDW_q. As an example, we depict in Fig. 3(a) the real-space density for CDW_π.

In Fig. 3(c), we can observe how the situation changes as we increase the value of V_p/V_h. If the amplitude of the

periodic potential is sufficiently large, a disordered phase emerges between the different CDW_q phases, where $S(q)$ vanishes at all momenta. This is an example of a frustrated phase [95], where the density order melts due to quantum fluctuations enhanced by competing interactions in a region where the different density orders are close in energy. Instead, a bond order develops [Fig. 3(a)], characterized by a nonzero value of the order parameter $B = 1/L \sum_j (-1)^j \langle \hat{B}_j \rangle$, with $\hat{B}_j = \hat{b}_j^\dagger \hat{b}_{j+1} + \text{H.c.}$ [Fig. 3(e)]. This bond-order wave (BOW) is a strongly correlated phase that cannot be accessed through the conventional RKKY interactions [63], since it requires comparable nearest and next-nearest neighbor interactions, while further-range interactions should vanish. This guarantees, in particular, that the classical energies corresponding to CDW_π and $CDW_{\pi/2}$ patterns are similar, thus enhancing frustration, while keeping the energy of CDW_q much higher. While this situation can be achieved for spinful fermions with dipolar interactions [96], spinless particles require $v_2/v_1 \approx 0.5$ [97], which is achieved here by varying the periodic potential, as shown previously. Similarly to the fermionic case [96], here the BOW phase possesses nontrivial topological properties. These are characterized by both a nonzero quantized value of a Berry phase [85,98] [Fig. 3(d)], and the emergence of localized protected states at the boundaries [Fig. 3(f)]. We note that similar topological effects are observed in nonfrustrated BOW phases induced instead by dynamical optical lattices [99–105].

Controlling the shape of the interactions.—Let us finally provide a way of tuning the interactions, which is unique in atomic systems, enabled by the possibility to control the effective dimensionality of the fermionic gas. In particular, by superimposing three independent standing-wave potentials, each ω_i in Eq. (1) can be controlled independently for the three orthogonal directions by modifying their intensity [see Fig. 1(d)]. Starting from $\omega_x = \omega_y = \omega_z$ and increasing ω_y, one can go smoothly from a 3D fermionic gas to an effective 2D one for $\omega_{x,z} \ll \omega_y/N$ [106,107]. Similarly, increasing ω_z connects the 2D and the 1D case. Since the power-law exponent of $F(r)$ depends on the dimension D as $1/r^D$, one expects that this method interpolates between different integer values.

We now explore the effect of this dimensional crossover in the effective interactions $F(r)$ for the two- to one-dimensional transition, while we maintain the bosons in 1D. Figure 4(a) shows $F(r)$ as a function of the anisotropy ratio $\omega_z/(\omega_x N)$ and $k_F d$, together with some cuts at the 1D-intermediate-2D regimes in Figs. 4(b)–4(d). Note that the dependence on N is introduced because the crossover is expected in the limit $\omega_z/\omega_x \sim N$, where the energy of the highest-energy state is not enough to induce an excitation in the z direction, and the interaction becomes effectively 1D. We observe that the interpolation is more intricate than initially expected. While in the limits $\omega_z/(\omega_x N) \gg (\ll)1$ one recovers the expected 1D (2D) RKKY-type
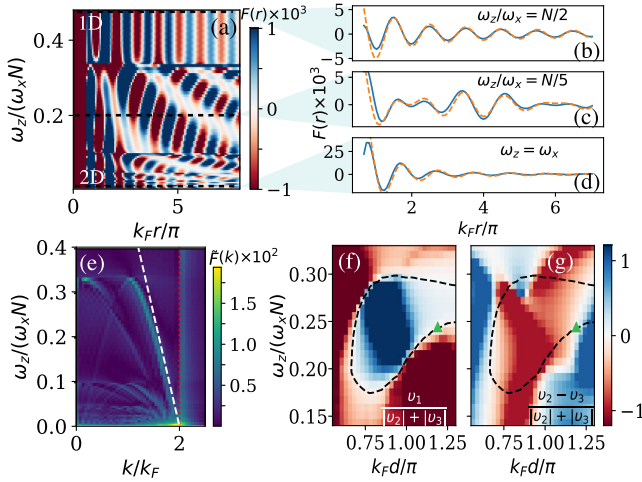
FIG. 4. (a) Mediated potential $F(r)$ as a function of the anisotropy ratio $\omega_z/(N\omega_x)$ and effective atomic separation $k_F r$. Repulsive (attractive) forces are represented in red (blue). (b)–(d) Value of $F(r)$ for three anisotropy ratios (blue) indicated in (a) with black dashed lines, compared to the expected analytical results [Eqs. (5) and (6)] (orange). (e) Cosine transform of $F(r)$ as a function of $\omega_z/(N\omega_x)$, where the dotted lines correspond to the frequencies $2k_F$ (red) and $\tilde{k}_1$ (white). (f), (g) Relation between the nearest-neighbor potentials $v_{1,2,3}$ of a kagome lattice with lattice spacing d, as a function of $\omega_z/(\omega_x N)$ and $k_F d$. Dashed contour follows $v_1 = 0$. Here, we took $N = 250$ and the rest of the parameters as in Fig. 2.

interactions, the intermediate dimensions acquire additional beating oscillations due to the presence of different harmonics in the potentials. This is more evident in Fig. 4(e), where we plot the corresponding cosine transform $\tilde{F}(k)$. The frequency $2k_F$ appears in all intermediate dimensions and, through a careful analysis, we observe that additional frequencies appear associated to discrete values $\tilde{k}_n = 2k_F[1 - n\omega_z/(\omega_x N)]$. The larger is the value of ω_z/ω_x, the smaller is the contribution associated to smaller frequencies (as longer effective lengths that cannot fit the constrained direction vanish). In particular, in the range $\omega_z/(\omega_x N) \in (0.1, 1/3)$, only contributions associated to $\tilde{k}_0$ and $\tilde{k}_1$ are dominant, leading to a smooth beating between the two frequencies in the potential, as we fit in Fig. 4(c) (dashed line). Such renormalization of the associated Friedel oscillations can also appear, e.g., due to the dressing with additional impurity atoms [74].

Despite the apparent complexity of the fermion-mediated interactions within this dimensional crossover, they might lead to the appearance of novel many-body phases difficult to obtain otherwise. For example, recent works have shown how chiral spin liquids can appear for hardcore bosons in kagome lattices with long-range interactions where the second and third neighbor terms are similar and the nearest neighbor interaction cancels, i.e., ($v_2 \approx v_3$ and $v_1 = 0$) [80], a regime that is typically hard to

access with conventional approaches. In Figs. 4(f) and 4(g), we make a search of whether such regime would be accessible through this dimensional crossover, and find that indeed there are configurations where $v_1 \approx 0$ (see contour line), while $v_2 \approx v_3$ (green marker). Although further analysis is required, especially to account for the effect of further-range interactions in the phase diagram, our results show a promising avenue to investigate magnetic frustration and spin liquids states in 2D ultracold atomic mixtures using tunable long-range interactions.

Conclusions.—We provide two strategies to control fermion-mediated interactions in ultracold atomic mixtures by modifying the fermionic confinement potential. First, we add an extra periodic potential to open a gap in the fermionic band. Then, we continuously modify the effective dimension of the fermionic gas by using anisotropic traps. In both cases, we characterize the emergent long-range interactions, obtaining a very versatile control over their range and shape. Finally, we consider different examples where this extended quantum simulation toolbox can lead to the exploration of frustrated quantum many-body phases that are not easily accessible with other approaches. Given the recent experiments in this direction [26,69], and the relatively simple tools that our proposal demands, we expect our results to guide near-future experiments on the topic.

*Corresponding author.
javier.arguello@icfo.eu
†Corresponding author.
a.gonzalez.tudela@csic.es
‡Corresponding author.
daniel.gonzalez-cuadra@uibk.ac.at

[1] H. P. Büchler and G. Blatter, Supersolid Versus Phase Separation in Atomic Bose-Fermi Mixtures, Phys. Rev. Lett. 91, 130404 (2003).

[2] V. W. Scarola and S. Das Sarma, Quantum Phases of the Extended Bose-Hubbard Hamiltonian: Possibility of a Supersolid State of Cold Atoms in Optical Lattices, Phys. Rev. Lett. 95, 033003 (2005).

[3] J. Léonard, A. Morales, P. Zupancic, T. Esslinger, and T. Donner, Supersolid formation in a quantum gas breaking a continuous translational symmetry, Nature (London) **543,** 87 (2017).

[4] L. Tanzi, E. Lucioni, F. Famà, J. Catani, A. Fioretti, C. Gabbanini, R. N. Bisset, L. Santos, and G. Modugno, Observation of a Dipolar Quantum Gas with Metastable Supersolid Properties, Phys. Rev. Lett. **122,** 130405 (2019).

[5] F. Böttcher, J.-N. Schmidt, M. Wenzel, J. Hertkorn, M. Guo, T. Langen, and T. Pfau, Transient Supersolid Properties in an Array of Dipolar Quantum Droplets, Phys. Rev. X **9,** 011051 (2019).

[6] L. Chomaz, D. Petter, P. Ilzhöfer, G. Natale, A. Trautmann, C. Politi, G. Durastante, R. M. W. van Bijnen, A. Patscheider, M. Sohmen, M. J. Mark, and F. Ferlaino, Long-Lived and Transient Supersolid Behaviors in Dipolar Quantum Gases, Phys. Rev. X **9,** 021012 (2019).

[7] A. Micheli, G. K. Brennen, and P. Zoller, A toolbox for lattice-spin models with polar molecules, Nat. Phys. **2,** 341 (2006).

[8] R. Barnett, D. Petrov, M. Lukin, and E. Demler, Quantum Magnetism with Multicomponent Dipolar Molecules in an Optical Lattice, Phys. Rev. Lett. **96,** 190401 (2006).

[9] A. V. Gorshkov, S. R. Manmana, G. Chen, J. Ye, E. Demler, M. D. Lukin, and A. M. Rey, Tunable Superfluidity and Quantum Magnetism with Ultracold Polar Molecules, Phys. Rev. Lett. **107,** 115301 (2011).

[10] M. Maik, P. Hauke, O. Dutta, J. Zakrzewski, and M. Lewenstein, Quantum spin models with long-range interactions and tunnelings: A quantum Monte Carlo study, New J. Phys. **14,** 113006 (2012).

[11] R. M. W. van Bijnen and T. Pohl, Quantum Magnetism and Topological Ordering via Rydberg Dressing Near Förster Resonances, Phys. Rev. Lett. **114,** 243002 (2015).

[12] A. W. Glaetzle, M. Dalmonte, R. Nath, C. Gross, I. Bloch, and P. Zoller, Designing Frustrated Quantum Magnets with Laser-Dressed Rydberg Atoms, Phys. Rev. Lett. **114,** 173002 (2015).

[13] S. R. Manmana, E. M. Stoudenmire, K. R. A. Hazzard, A. M. Rey, and A. V. Gorshkov, Topological phases in ultracold polar-molecule quantum magnets, Phys. Rev. B **87,** 081106(R) (2013).

[14] N. Y. Yao, A. V. Gorshkov, C. R. Laumann, A. M. Läuchli, J. Ye, and M. D. Lukin, Realizing Fractional Chern Insulators in Dipolar Spin Systems, Phys. Rev. Lett. **110,** 185302 (2013).

[15] N. Y. Yao, M. P. Zaletel, D. M. Stamper-Kurn, and A. Vishwanath, A quantum dipolar spin liquid, Nat. Phys. **14,** 405 (2018).

[16] S. de Léséleuc, V. Lienhard, P. Scholl, D. Barredo, S. Weber, N. Lang, H. P. Büchler, T. Lahaye, and A. Browaeys, Observation of a symmetry-protected topological phase of interacting bosons with Rydberg atoms, Science **365,** 775 (2019).

[17] R. Samajdar, W. W. Ho, H. Pichler, M. D. Lukin, and S. Sachdev, Quantum phases of rydberg atoms on a kagome lattice, Proc. Natl. Acad. Sci. U.S.A. **118,** e2015785118 (2021).

[18] R. Verresen, M. D. Lukin, and A. Vishwanath, Prediction of Toric Code Topological Order from Rydberg Blockade, Phys. Rev. X **11,** 031005 (2021).

[19] G. Semeghini, H. Levine, A. Keesling, S. Ebadi, T. T. Wang, D. Bluvstein, R. Verresen, H. Pichler, M. Kalinowski, R. Samajdar, A. Omran, S. Sachdev, A. Vishwanath, M. Greiner, V. Vuletić, and M. D. Lukin, Probing topological spin liquids on a programmable quantum simulator, Science **374,** 1242 (2021).

[20] D. González-Cuadra, Higher-order topological quantum paramagnets, Phys. Rev. B **105,** L020403 (2022).

[21] J. Fraxanet, D. González-Cuadra, T. Pfau, M. Lewenstein, T. Langen, and L. Barbiero, Topological Quantum Critical Points in the Extended Bose-Hubbard Model, Phys. Rev. Lett. **128,** 043402 (2022).

[22] M. Bello, G. Platero, J. I. Cirac, and A. González-Tudela, Unconventional quantum optics in topological waveguide QED, Sci. Adv. **5,** eaaw0297 (2019).

[23] M. Bello, G. Platero, and A. González-Tudela, Spin many-body phases in standard- and topological-waveguide QED simulators, PRX Quantum **3,** 010336 (2022).

[24] T. Karpiuk, M. Brewczyk, S. Ospelkaus-Schwarzer, K. Bongs, M. Gajda, and K. Rzążewski, Soliton Trains in Bose-Fermi Mixtures, Phys. Rev. Lett. **93,** 100401 (2004).

[25] J. Santhanam, V. M. Kenkre, and V. V. Konotop, Solitons of Bose-Fermi mixtures in a strongly elongated trap, Phys. Rev. A **73,** 013612 (2006).

[26] B. J. DeSalvo, K. Patel, G. Cai, and C. Chin, Observation of fermion-mediated interactions between bosonic atoms, Nature (London) **568,** 61 (2019).

[27] P. Cheiney, C. R. Cabrera, J. Sanz, B. Naylor, L. Tanzi, and L. Tarruell, Bright Soliton to Quantum Droplet Transition in a Mixture of Bose-Einstein Condensates, Phys. Rev. Lett. **120,** 135301 (2018).

[28] I. Ferrier-Barbut, H. Kadau, M. Schmitt, M. Wenzel, and T. Pfau, Observation of Quantum Droplets in a Strongly Dipolar Bose Gas, Phys. Rev. Lett. **116,** 215301 (2016).

[29] L. Chomaz, S. Baier, D. Petter, M. J. Mark, F. Wächtler, L. Santos, and F. Ferlaino, Quantum-Fluctuation-Driven Crossover from a Dilute Bose-Einstein Condensate to a Macrodroplet in a Dipolar Quantum Fluid, Phys. Rev. X **6,** 041039 (2016).

[30] C. R. Cabrera, L. Tanzi, J. Sanz, B. Naylor, P. Thomas, P. Cheiney, and L. Tarrue, Quantum liquid droplets in a mixture of bose-Einstein condensates, Science **359,** 301 (2018).

[31] R. Mottl, F. Brennecke, K. Baumann, R. Landig, T. Donner, and T. Esslinger, Roton-type mode softening in a quantum gas with cavity-mediated long-range interactions, Science **336,** 1570 (2012).

[32] C. Feng and Y. Chen, Tunable range interactions and multi-roton excitations for bosons in a Bose-Fermi mixture with optical lattices, Commun. Theor. Phys. **71,** 869 (2019).

[33] J. Argüello-Luengo, A. González-Tudela, T. Shi, P. Zoller, and J. Cirac, Analogue quantum chemistry simulation, Nature (London) **574,** 215 (2019).

[34] J. Argüello-Luengo, A. González-Tudela, T. Shi, P. Zoller, and J. Ignacio Cirac, Quantum simulation of 2D quantum

chemistry in optical lattices, Phys. Rev. Research **2,** 042013(R) (2020).

[35] J. Argüello-Luengo, T. Shi, and A. González-Tudela, Engineering analog quantum chemistry Hamiltonians using cold atoms in optical lattices, Phys. Rev. A **103,** 043318 (2021).

[36] E. Zohar, J. I. Cirac, and B. Reznik, Quantum simulations of lattice gauge theories using ultracold atoms in optical lattices, Rep. Prog. Phys. **79,** 014401 (2015).

[37] M. C. Bañuls, R. Blatt, J. Catani, A. Celi, J. I. Cirac, M. Dalmonte, L. Fallani, K. Jansen, M. Lewenstein, S. Montangero, C. A. Muschik, B. Reznik, E. Rico, L. Tagliacozzo, K. Van Acoleyen, F. Verstraete, U.-J. Wiese, M. Wingate, J. Zakrzewski, and P. Zoller, Simulating lattice gauge theories within quantum technologies, Eur. Phys. J. D **74,** 165 (2020).

[38] D. González-Cuadra, A. Dauphin, M. Aidelsburger, M. Lewenstein, and A. Bermudez, Rotor Jackiw-Rebbi model: A cold-atom approach to chiral symmetry restoration and charge confinement, PRX Quantum **1,** 020321 (2020).

[39] M. Aidelsburger *et al.*, Cold atoms meet lattice gauge theory, Phil. Trans. R. Soc. A **380,** 20210064 (2022).

[40] J. Bloch, B. Sermage, M. Perrin, P. Senellart, R. André, and Le Si Dang, Monitoring the dynamics of a coherent cavity polariton population, Phys. Rev. B **71,** 155311 (2005).

[41] M. Lu, N. Q. Burdick, S. H. Youn, and B. L. Lev, Strongly Dipolar Bose-Einstein Condensate of Dysprosium, Phys. Rev. Lett. **107,** 190401 (2011).

[42] S. Giovanazzi, A. Görlitz, and T. Pfau, Tuning the Dipolar Interaction in Quantum Gases, Phys. Rev. Lett. **89,** 130401 (2002).

[43] A. Griesmaier, J. Werner, S. Hensler, J. Stuhler, and T. Pfau, Bose-Einstein Condensation of Chromium, Phys. Rev. Lett. **94,** 160401 (2005).

[44] J. Zeiher, R. Van Bijnen, P. Schauß, S. Hild, J.-y. Choi, T. Pohl, I. Bloch, and C. Gross, Many-body interferometry of a Rydberg-dressed spin lattice, Nat. Phys. **12,** 1095 (2016).

[45] E. Guardado-Sanchez, P. T. Brown, D. Mitra, T. Devakul, D. A. Huse, P. Schauß, and W. S. Bakr, Probing the Quench Dynamics of Antiferromagnetic Correlations in a 2D Quantum Ising Spin System, Phys. Rev. X **8,** 021069 (2018).

[46] V. Lienhard, S. de Léséleuc, D. Barredo, T. Lahaye, A. Browaeys, M. Schuler, L. P. Henry, and A. M. Läuchli, Observing the Space- and Time-Dependent Growth of Correlations in Dynamically Tuned Synthetic Ising Models with Antiferromagnetic Interactions, Phys. Rev. X **8,** 021070 (2018).

[47] A. Browaeys and T. Lahaye, Many-body physics with individually controlled Rydberg atoms, Nat. Phys. **16,** 132 (2020).

[48] K. K. Ni, S. Ospelkaus, M. H. De Miranda, A. Pe'er, B. Neyenhuis, J. J. Zirbel, S. Kotochigova, P. S. Julienne, D. S. Jin, and J. Ye, A high phase-space-density gas of polar molecules, Science **322,** 231 (2008).

[49] J. Deiglmayr, A. Grochola, M. Repp, K. Mörtlbauer, C. Glück, J. Lange, O. Dulieu, R. Wester, and M. Weidemüller, Formation of Ultracold Polar Molecules in the Rovibrational Ground State, Phys. Rev. Lett. **101,** 133004 (2008).

[50] J. Stuhler, A. Griesmaier, T. Koch, M. Fattori, T. Pfau, S. Giovanazzi, P. Pedri, and L. Santos, Observation of Dipole-Dipole Interaction in a Degenerate Quantum Gas, Phys. Rev. Lett. **95,** 150406 (2005).

[51] K. R. A. Hazzard, B. Gadway, M. Foss-Feig, B. Yan, S. A. Moses, J. P. Covey, N. Y. Yao, M. D. Lukin, J. Ye, D. S. Jin, and A. M. Rey, Many-Body Dynamics of Dipolar Molecules in an Optical Lattice, Phys. Rev. Lett. **113,** 195302 (2014).

[52] K. Baumann, C. Guerlin, F. Brennecke, and T. Esslinger, Dicke quantum phase transition with a superfluid gas in an optical cavity, Nature (London) **464,** 1301 (2010).

[53] P. Münstermann, T. Fischer, P. Maunz, P. W. H. Pinkse, and G. Rempe, Observation of Cavity-Mediated Long-Range Light Forces between Strongly Coupled Atoms, Phys. Rev. Lett. **84,** 4068 (2000).

[54] H. Ritsch, P. Domokos, F. Brennecke, and T. Esslinger, Cold atoms in cavity-generated dynamical optical potentials, Rev. Mod. Phys. **85,** 553 (2013).

[55] V. D. Vaidya, Y. Guo, R. M. Kroeze, K. E. Ballantine, A. J. Kollár, J. Keeling, and B. L. Lev, Tunable-Range, Photon-Mediated Atomic Interactions in Multimode Cavity QED, Phys. Rev. X **8,** 011002 (2018).

[56] J. S. Douglas, H. Habibian, C.-L. Hung, A. V. Gorshkov, H. J. Kimble, and D. E. Chang, Quantum many-body models with cold atoms coupled to photonic crystals, Nat. Photonics **9,** 326 (2015).

[57] A. González-Tudela, C.-L. Hung, D. Chang, J. Cirac, and H. Kimble, Subwavelength vacuum lattices and atom-atom interactions in two-dimensional photonic crystals, Nat. Photonics **9,** 320 (2015).

[58] D. E. Chang, J. S. Douglas, A. González-Tudela, C.-L. Hung, and H. J. Kimble, Colloquium: Quantum matter built from nanoscopic lattices of atoms and photons, Rev. Mod. Phys. **90,** 031002 (2018).

[59] S. T. Chui and V. N. Ryzhov, Collapse transition in mixtures of bosons and fermions, Phys. Rev. A **69,** 043607 (2004).

[60] K. Günter, T. Stöferle, H. Moritz, M. Köhl, and T. Esslinger, Bose-Fermi Mixtures in a Three-Dimensional Optical Lattice, Phys. Rev. Lett. **96,** 180402 (2006).

[61] S. Sinha and K. Sengupta, Phases and collective modes of a hardcore Bose-Fermi mixture in an optical lattice, Phys. Rev. B **79,** 115124 (2009).

[62] T. Best, S. Will, U. Schneider, L. Hackermüller, D. van Oosten, I. Bloch, and D. S. Lühmann, Role of Interactions in Rb87-K40 Bose-Fermi Mixtures in a 3D Optical Lattice, Phys. Rev. Lett. **102,** 030408 (2009).

[63] A. Mering and M. Fleischhauer, Fermion-mediated long-range interactions of bosons in the one-dimensional bose-fermi-hubbard model, Phys. Rev. A **81,** 011603(R) (2010).

[64] T. P. Polak and T. K. Kopeć, Zero-temperature phase diagram of Bose-Fermi gaseous mixtures in optical lattices, Phys. Rev. A **81,** 043612 (2010).

[65] I. Ferrier-Barbut, M. Delehaye, S. Laurent, A. T. Grier, M. Pierce, B. S. Rem, F. Chevy, and C. Salomon, A mixture of Bose and Fermi superfluids, Science **345,** 1035 (2014).

[66] S. De and I. B. Spielman, Fermion-mediated long-range interactions between bosons stored in an optical lattice, Appl. Phys. B **114,** 527 (2014).

[67] D. Suchet, Z. Wu, F. Chevy, and G. M. Bruun, Long-range mediated interactions in a mixed-dimensional system, Phys. Rev. A 95, 043643 (2017).

[68] B. J. DeSalvo, K. Patel, J. Johansen, and C. Chin, Observation of a Degenerate Fermi Gas Trapped by a Bose-Einstein Condensate, Phys. Rev. Lett. 119, 233401 (2017).

[69] H. Edri, B. Raz, N. Matzliah, N. Davidson, and R. Ozeri, Observation of Spin-Spin Fermion-Mediated Interactions between Ultracold Bosons, Phys. Rev. Lett. 124, 163401 (2020).

[70] D. C. Zheng, C. R. Ye, L. Wen, and R. Liao, Polarizing the medium: Fermion-mediated interactions between bosons, Phys. Rev. A 103, L021301 (2021).

[71] J. N. Fuchs, A. Recati, and W. Zwerger, Oscillating Casimir force between impurities in one-dimensional Fermi liquids, Phys. Rev. A 75, 043615 (2007).

[72] A. Recati, J. N. Fuchs, C. S. Peça, and W. Zwerger, Casimir forces between defects in one-dimensional quantum liquids, Phys. Rev. A 72, 023616 (2005).

[73] P. Wächter, V. Meden, and K. Schönhammer, Indirect forces between impurities in one-dimensional quantum liquids, Phys. Rev. B 76, 045123 (2007).

[74] M. Maslov, M. Lemeshko, and A. G. Volosniev, Impurity with a resonance in the vicinity of the Fermi energy, Phys. Rev. Research 4, 013160 (2022).

[75] D. Huber, H. W. Hammer, and A. G. Volosniev, In-medium bound states of two bosonic impurities in a one-dimensional Fermi gas, Phys. Rev. Research 1, 033177 (2019).

[76] D. H. Santamore and E. Timmermans, Fermion-mediated interactions in a dilute Bose-Einstein condensate, Phys. Rev. A 78, 013619 (2008).

[77] T. Kasuya, A theory of metallic ferro- and antiferro-magnetism on Zener's model, Prog. Theor. Phys. 16, 45 (1956).

[78] M. A. Ruderman and C. Kittel, Indirect exchange coupling of nuclear magnetic moments by conduction electrons, Phys. Rev. 96, 99 (1954).

[79] K. Yosida, Magnetic properties of Cu-Mn alloys, Phys. Rev. 106, 893 (1957).

[80] W. Zhu, S. S. Gong, and D. N. Sheng, Interaction-driven fractional quantum Hall state of hard-core bosons on kagome lattice at one-third filling, Phys. Rev. B 94, 035129 (2016).

[81] C. Chin, R. Grimm, P. Julienne, and E. Tiesinga, Feshbach resonances in ultracold gases, Rev. Mod. Phys. 82, 1225 (2010).

[82] Q. D. Jiang, On the sign of fermion-mediated interactions, Phys. Rev. B 103, L121107 (2021).

[83] T. M. Rusin and W. Zawadzki, On calculation of RKKY range function in one dimension, J. Magn. Magn. Mater. 441, 387 (2017).

[84] B. Fischer and M. W. Klein, Magnetic and nonmagnetic impurities in two-dimensional metals, Phys. Rev. B 11, 2025 (1975).

[85] See Supplemental Material at http://link.aps.org/supplemental/10.1103/PhysRevLett.129.083401, which includes Refs. [86–93], for further details on the experimental implementation, as well as on the calculation of the mediated potential and the topological Berry phase.

[86] C. Silber, S. Günther, C. Marzok, B. Deh, P. W. Courteille, and C. Zimmermann, Quantum-Degenerate Mixture of Fermionic Lithium and Bosonic Rubidium Gases, Phys. Rev. Lett. 95, 170408 (2005).

[87] B. J. DeSalvo, K. Patel, J. Johansen, and C. Chin, Observation of a Degenerate Fermi Gas Trapped by a Bose-Einstein Condensate, Phys. Rev. Lett. 119, 233401 (2017).

[88] L. Hruby, N. Dogra, M. Landini, T. Donner, and T. Esslinger, Metastability and avalanche dynamics in strongly correlated gases with long-range interactions, Proc. Natl. Acad. Sci. U.S.A. 115, 3279 (2018).

[89] M. Schecter and A. Kamenev, Phonon-Mediated Casimir Interaction between Mobile Impurities in One-Dimensional Quantum Liquids, Phys. Rev. Lett. 112, 155301 (2014).

[90] A. Galindo and P. Pascual, Quantum Mechanics I (Springer Science & Business Media, New York, 2012).

[91] M. Abramowitz and I. A. Stegun, Handbook of Mathematical Functions with Formulas, Graphs and Mathematical Tables, 9th printing (Dover, New York, 1972).

[92] D. Xiao, M.-C. Chang, and Q. Niu, Berry phase effects on electronic properties, Rev. Mod. Phys. 82, 1959 (2010).

[93] M. P. Zaletel, R. S. K. Mong, and F. Pollmann, Flux insertion, entanglement, and quantized responses, J. Stat. Mech. (2014) P10007.

[94] J. Hauschild and F. Pollmann, Efficient numerical simulations with Tensor Networks: Tensor Network Python (TeNPy), SciPost Phys. Lect. Notes 5 (2018), 10.21468/SciPostPhysLectNotes.5.

[95] C. Lacroix, P. Mendels, and F. Mila, Introduction to Frustrated Magnetism: Materials, Experiments, Theory (Springer Science & Business Media, New York, 2011), Vol. 164.

[96] S. Julià-Farré, D. González-Cuadra, A. Patscheider, M. J. Mark, F. Ferlaino, M. Lewenstein, L. Barbiero, and A. Dauphin, Revealing the topological nature of the bond order wave in a strongly correlated quantum system, arXiv:2112.08785.

[97] T. Mishra, J. Carrasquilla, and M. Rigol, Phase diagram of the half-filled one-dimensional $t - v - V'$ model, Phys. Rev. B 84, 115135 (2011).

[98] Y. Hatsugai, Quantized berry phases as a local order parameter of a quantum liquid, J. Phys. Soc. Jpn. 75, 123601 (2006).

[99] D. González-Cuadra, P. R. Grzybowski, A. Dauphin, and M. Lewenstein, Strongly Correlated Bosons on a Dynamical Lattice, Phys. Rev. Lett. 121, 090402 (2018).

[100] D. González-Cuadra, A. Dauphin, P. R. Grzybowski, P. Wójcik, M. Lewenstein, and A. Bermudez, Symmetry-breaking topological insulators in the $\mathbb{z}_2$ bose-hubbard model, Phys. Rev. B 99, 045139 (2019).

[101] D. González-Cuadra, A. Bermudez, P. R. Grzybowski, M. Lewenstein, and A. Dauphin, Intertwined topological phases induced by emergent symmetry protection, Nat. Commun. 10, 2694 (2019).

[102] D. González-Cuadra, A. Dauphin, P. R. Grzybowski, M. Lewenstein, and A. Bermudez, Dynamical Solitons and Boson Fractionalization in Cold-Atom Topological Insulators, Phys. Rev. Lett. **125**, 265301 (2020).

[103] D. González-Cuadra, A. Dauphin, P. R. Grzybowski, M. Lewenstein, and A. Bermudez, $\mathbb{z}_n$ solitons in intertwined topological phases, Phys. Rev. B **102**, 245137 (2020).

[104] T. Chanda, R. Kraus, G. Morigi, and J. Zakrzewski, Self-organized topological insulator due to cavity-mediated correlated tunneling, Quantum **5**, 501 (2021).

[105] T. Chanda, D. González-Cuadra, M. Lewenstein, L. Tagliacozzo, and J. Zakrzewski, Devil's staircase of topological Peierls insulators and Peierls supersolids, SciPost Phys. **12**, 76 (2022).

[106] P. Dyke, E. D. Kuhnle, S. Whitlock, H. Hu, M. Mark, S. Hoinka, M. Lingham, P. Hannaford, and C. J. Vale, Crossover from 2D to 3D in a Weakly Interacting Fermi Gas, Phys. Rev. Lett. **106**, 105304 (2011).

[107] K. Martiyanov, V. Makhalov, and A. Turlapov, Observation of a Two-Dimensional Fermi Gas of Atoms, Phys. Rev. Lett. **105**, 030404 (2010).